

A physical interpretation of the variability power spectral components in accreting black holes and neutron stars

Adam Ingram^{1*} & Chris Done¹

¹*Department of Physics, University of Durham, South Road, Durham DH1 3LE, UK*

Submitted to MNRAS

ABSTRACT

We propose a physical framework for interpreting the broad band power spectra from black hole and neutron star binaries. We use the truncated disc/hot inner flow geometry, and assume that the hot flow is generically turbulent. Each radius in the hot flow produces fluctuations, and we further assume that these are damped on the viscous frequency. Integrating over radii gives broad band continuum noise power between low and high frequency breaks which are set by the viscous timescale at the outer and inner edge of the hot flow, respectively. Lense-Thirring (vertical) precession of the entire hot flow superimposes the low frequency QPO on this continuum power.

We test this model on the power spectra seen in the neutron star systems (atolls) as these have the key advantage that the (upper) kHz QPO most likely independently tracks the truncation radius. These show that this model can give a consistent solution, with the truncation radius decreasing from $20 - 8R_g$ while the inner radius of the flow remains remarkably constant at $6 R_g$. This very constrained geometry still does not quite completely determine the Lense-Thirring precession frequency as this also depends on the radial distribution of mass in the hot flow. Nonetheless, we show that this can be consistent with the low frequency QPO, showing that the broad band power spectra can be used as a diagnostic of accretion flows in strong gravity.

Key words: X-rays: binaries – accretion, accretion discs

1 INTRODUCTION

Black holes and neutron stars have very similar gravitational potentials as neutron star radii are approximately the size of the last stable orbit. Thus their accretion flows should be similar despite the fundamental difference in the nature of the central object: neutron stars have a solid surface, while black holes do not. This similarity is seen in the spectral and timing properties. Both black hole binaries (BHB) and disc accreting neutron stars (atolls) show a distinct transition between hard spectra seen at low luminosities (termed the low/hard state in BHB and the island state in atolls) and much softer spectra seen at high luminosities (high/soft in BHB, banana branch in atolls). During the transition, the properties of the rapid variability also change. This variability can be approximately described as band limited continuum noise between a low and high frequency break, with a low frequency Quasi-Periodic Oscillation (hereafter LF QPO) superimposed. The low frequency break and LF QPO move to higher frequencies as the source spectrum softens in both BHB and atolls (see e.g. the reviews by van der Klis 2005,

hereafter vdK05; McClintock & Remillard 2006, hereafter MR06; and Done, Gierlinski & Kubota 2007, hereafter DGK07)

Both spectral and variability behaviour can be qualitatively explained if the geometrically thin, cool accretion disc is replaced at radius r_o by a hot inner flow which produces the hard Comptonised spectrum. As this transition radius decreases, the disc spectrum increases in luminosity and temperature and more soft seed photons from the disc illuminate the corona. This increases the Compton cooling so the hard spectrum softens slightly. This effect becomes much stronger when the disc extends far enough down in radii to overlap with the hot flow, and the Comptonised spectrum softens dramatically with decreasing radius as the disc approaches the last stable orbit. Throughout this evolution, all the timescales for variability associated with the inner edge of the thin disc decrease. This explains the correlated spectral-timing behaviour observed in both BHB and atolls if the low frequency break and LF QPO are set by r_o (Barret 2001; DGK07).

Nonetheless, there are also differences in behaviour between the BHB and atolls which must be tied to the fundamental difference in nature of the compact object. Spectrally, the atolls show a clear additional component from an optically thick boundary layer between the disc and solid neutron star surface at high luminosi-

* E-mail: a.r.ingram@durham.ac.uk

ties (Barret 2001; DGK07). This boundary layer emission becomes (marginally) optically thin at lower luminosities, giving rise to the hard island state (Barret et al 2000) but it is still plainly present in terms of additional variability power at high frequencies (Sunyaev & Revnivtsev 2000; DGK07). The atolls also show kHz QPOs which are much stronger and much more coherent than any equivalent features which may be present in the BHB (vdK05).

While there have been some quantitative tests of the spectral evolution of the disc and hot flow predicted by these models (Chaty et al 2003; Gierliński, Done, & Page 2008; Cabanac et al 2008), there has been no comparable test using the variability properties as their fundamental components are not yet understood. This is especially evident in the case of the LF QPO. This is a clear characteristic frequency, most probably associated with r_o , yet it cannot be used to quantitatively determine r_o until its physical origin is known. While there are a plethora of potential mechanisms in the literature (e.g. Fragile et al 2001; vdK05), our recent model of Lense-Thirring (vertical) precession of the hot inner flow is the first to simultaneously explain both its timing and spectral properties (Ingram, Done & Fragile 2009, hereafter IDF09).

Lense-Thirring precession is a relativistic effect whereby a spinning black hole with its angular momentum misaligned with that of the binary system produces a torque. This propagates via bending waves throughout the hot flow, and can make the entire flow within r_o vertically precess as a solid body (though it does not *rotate* as a solid body: orbits are still approximately Keplerian). The precession frequency is set by the outer radius of the vertically precessing flow, r_o , the dimensionless black hole spin parameter, a_* , and the inner radius of the hot flow, r_i , for a given mass, M . The precession frequency of the flow increases as r_o decreases until $r_o \rightarrow r_i$ when the thin disc extends underneath the hot flow at all radii, suppressing vertical modes. IDF09 used the qualitative constraint that all the spectral softening occurs as r_o decreases from $50 R_g \rightarrow r_i$ (where $R_g = GM/c^2$) to show that this model gives a good match to the observed LF QPO behaviour for BHB as a class.

Here we develop a full model for the power spectrum, encompassing the broad band noise as well as the LF QPO. Numerical simulations now give some insight into the nature of the noise generating process. Angular momentum transport in the accretion flow takes place via stresses (a.k.a. ‘viscosity’) generated by the Magneto-Rotational Instability (MRI: Balbus & Hawley 1998). This process generates a white noise of fluctuations in all quantities (e.g. Krolik & Hawley 2002). However, the mass accretion rate at any given radius cannot change faster than the local viscous timescale, so fluctuations at each radius are damped on this timescale (Lyubarskii 1997; Psaltis & Norman 2000; also see Misra & Zdziarski 2008 for a slightly different approach). Coupling this to the truncated disc/hot flow geometry gives a prediction of self-similar fluctuation power between timescales corresponding to the viscous timescale at the inner and outer radii of the hot flow (Titarchuk et al 2007; Churazov et al 2001). Thus the evolution of the continuum power spectrum can determine the inner and outer radii of the flow, and these can be used to *predict* the LF QPO frequency, to compare with that observed.

While we could do this in the BHB systems, the atolls give additional constraints as the spin of the neutron star is often independently known from burst oscillations (e.g. Strohmayer, Markwardt, & Kuulkers 2008; Piro & Bildsten 2005), and the derived values of the outer radius can be checked via the kHz QPOs. It is generally assumed that the upper kHz QPO (ukHz QPO) is the Keplerian frequency at the truncation radius r_o (e.g. van der Klis et al 1996; Stella & Vietri 1998; Schnittman 2005). The narrowness of

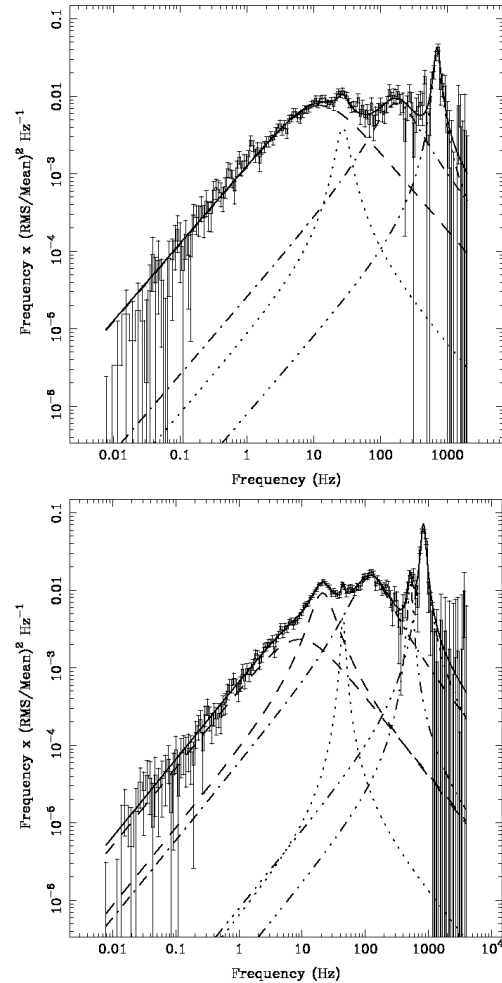


Figure 1. Power spectra and fit functions for 4U 1728-34 (top) and 4U 0614+09 (bottom), reproduced with the permission of van Straaten et al (2002) and the AAS. Lorentzians represent the following components: the lower break L_b (dashed), the LF QPO (dotted), the upper break L_u (dot-dashed) and the kHz QPOs (triple dot-dashed). When there are two dashed lines present, as in the bottom panel, we will refer to the left hand one as L_{b2} and the right hand one as L_{VLF} with one assumed to be a continuation of L_b .

the feature means that this gives an unambiguous determination of r_o . Hence here we use the atolls to outline a self-consistent model for *all* the observed components in the power spectrum.

2 THE ORIGIN OF THE BROAD BAND POWER SPECTRUM

We choose atoll sources with multiple observations showing the power spectral evolution so as to test the model over a wide range of r_o . We consider only low spin systems ($a_* < 0.3$), because higher spins lead to an equatorial bulge of the neutron star which distorts space-time from being well described by the Kerr metric (Miller et al 1998). This leads us to pick the atoll systems 4U 1728-34 and 4U 0614+09 (van Straaten et al 2002), both of which have spin $a_* \sim 0.2$ and mass $M \sim 1.4M_\odot$.

Typical power spectra of 4U 1728-34 and 4U 0614+09 are shown in the top and bottom panels respectively of Figure 1. We see that the QPOs described above are superimposed on a complex,

broad band noise continuum. This can be approximately modelled by a twice broken power law, following $P(\nu) \propto \nu^0$ below the lower break frequency ν_b , $P(\nu) \propto \nu^{-2}$ above the higher break frequency ν_u and $P(\nu) \propto \nu^{-1}$ between (i.e a flat top in $\nu P(\nu)$). However, multiple Lorentzians give a much better description of the broad band noise (Belloni, Psaltis & van der Klis 2002; Fig 1). Each of these has a characteristic frequency, ν_c , and width, $\Delta\nu$, which can be combined together into a quality factor $Q = \nu_c/\Delta\nu$. The lowest frequency component, L_b , is generally a zero centred Lorentzian, so it peaks in $\nu P(\nu)$ at $\Delta\nu$, producing the low frequency ‘break’ in the flat top noise. This break frequency correlates with the LF QPO and kHz QPOs (Wijnands & van der Klis 1999; Klein-Wolt & van der Klis 2008; Psaltis, Belloni & van der Klis 1999) whereas the high frequency ‘break’ (sometimes referred to as the hectohertz QPO) varies much less (e.g. vdK05; DGK07).

2.1 Outer radius

This behaviour of the high and low frequency breaks can be qualitatively explained in the truncated disc/hot inner flow model. The inner radius of the flow remains constant close to the neutron star radius, so giving the constant high frequency power, while the outer radius sweeps inwards, leading to the progressive loss of low frequency components (Gierlinski, Nikolajuk & Czerny 2008). Quantitatively this can be modelled by each radius generating noise power as a zero centred Lorentzian with width $\Delta\nu = 1/t_{visc} = 1.5\alpha(h/r)^2\nu_k(r)$, where α is the Shakura-Sunyaev viscosity parameter and h/r is the disc semi-thickness. However, this means that the low frequency break is dependent on $\alpha(h/r)^2$ as well as on r_o . This is unlike the LF QPO model of IDF09, which depends primarily on r_o , has a weak dependence on h/r via r_i , and has no dependence on α .

Simulation results clearly show that there is a marked increase in stress with radius due to the additional torque from a misaligned flow, increasing the effective α at small radii (Fragile et al 2007; 2009). These simulations also have h/r remaining fairly constant at ~ 0.2 over the body of the flow, but it seems more likely that h/r depends on mass accretion rate, especially in the atolls as the hot flow is collapsing into a narrow boundary layer. Thus we cannot determine r_o unambiguously from the low frequency break.

Instead, we can use additional information from the kHz QPOs to determine r_o assuming that $\nu_{ukHz} = \nu_k(r_o) = c/[2\pi R_g(r_o^{3/2} + a_*)]$. The top panel of Figure 2 shows that this requires r_o to decrease from 20 – $8R_g$, consistent with the expected change in radius from the spectral softening seen from the island state to the lower banana branch (Barret 2001). Thus the kHz QPOs disappear before the disc reaches the last stable orbit, which rules out models in which the decrease in coherence and power in the kHz QPOs at their highest frequencies is a signature of the last stable orbit (e.g. Barret et al 2005). Instead it seems more likely that the loss of coherence and power comes from scattering in the increasingly optically thick boundary layer (Mendez 2006).

This determination of r_o allows us to infer the required change in $\alpha(h/r)^2$ in order for this to be consistent with the observed low frequency break. The black points in the bottom panel of Figure 2 show this for data where ν_b is unambiguously identified in the power spectra. However, this becomes difficult at the highest kHz QPO frequencies (i.e. smallest radii) as there is an additional component observed in the low frequency power spectrum e.g. the lower panel of Figure 1, where two low frequency Lorentzians are required. It is not immediately clear which one of these corresponds

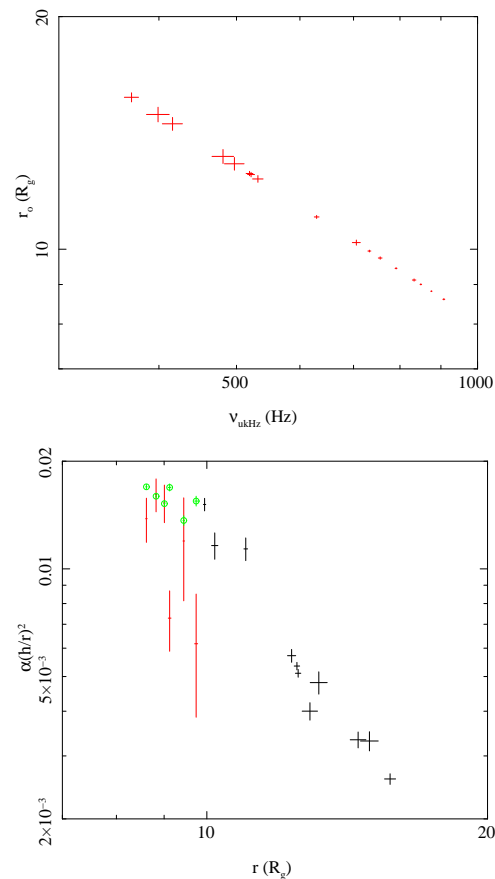


Figure 2. The top plot shows the relationship between r_o and ν_{ukHz} resulting from the assumption $\nu_{ukHz} = \nu_k(r_o)$. In the bottom panel, the product $\alpha(h/r)^2$ is plotted against r as implied by assuming that the break frequency is the viscous frequency at r_o . The black points are for power spectra where there is no ambiguity over what the break frequency is whereas the red points are for $\nu_b = \nu_{b2}$ and the green points for $\nu_b = \nu_{VLF}$.

to ν_b e.g. van Straaten et al (2002) refer to the lowest frequency Lorentzian as L_b and call the other L_{VLF} while Altamirano et al (2008) put L_b on the right and term the other L_{b2} . Here we only use L_b where this break is unambiguously determined by the data. Where there are two competing low frequency components we refer to the lowest frequency one as L_{b2} and the other as L_{VLF} . We take each of these in turn and derive their constraints on $\alpha(h/r)^2$ given r_o determined from the kHz QPO as shown by the green ($\nu_{VLF} = \nu_{visc}(r_o)$) and red ($\nu_{b2} = \nu_{visc}(r_o)$) points in Figure 2. The green points connect smoothly onto the black points where ν_b is unambiguously determined, while the red points do not. Thus it seems most likely that the higher of the two low frequency components represents the continuation of the break frequency determined by r_o .

What then is the origin of the lowest frequency component? Intriguingly, the geometry inferred from models of the spectral evolution require an *overlap* between the hot flow and truncated disc close to the transition. The splitting of the break frequency then has an obvious interpretation with the outer radius of the hot flow being larger than the inner radius of the thin disc. The hot flow in this overlap region will have smaller scale fluctuations, as the size scale of the magnetic field is limited by the thin disc in the mid plane.

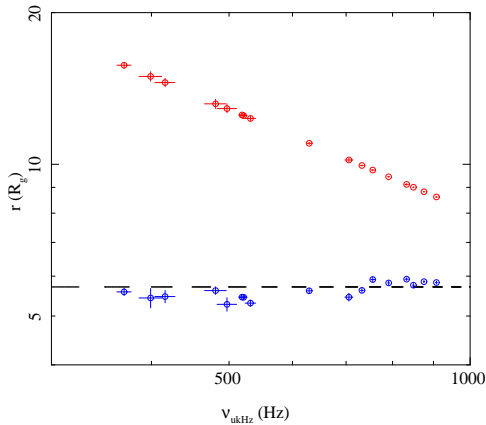


Figure 3. Plot showing how characteristic radii in the flow change as the ukHz QPO frequency increases for sources 4U 1728-34 and 4U 0614+09. The red points track the implied value of r_o from Figure 2. The blue points track the implied value of r_i and the black line traces out the bending wave radius from IDF09 which, for $a_* = 0.2$, coincides with the neutron star radius.

Thus this section of the flow provides a slightly lower variability power, making it distinct from the flow within r_o .

2.2 Inner radius

Using the ukHz QPO to determine the inner radius of the thin disc, r_o , shows that the stresses must increase with decreasing radius if r_o also sets the low frequency break. We can fit the black and green points in Figure 2 with the power law $\alpha(h/r)^2 \sim 10.4r^{-3}$. Using this relation, we are then able to determine the inner radius of the flow, r_i , under the assumption that the high frequency break, ν_u , is set by the viscous frequency at r_i .

$$r_i \approx \left(\frac{3c\alpha(h/r)^2}{4\pi R_g \nu_u} \right)^{2/3} \approx \left(\frac{7.8c}{\pi R_g \nu_u} \right)^{2/9}. \quad (1)$$

Figure 3 shows that this inner radius remains remarkably constant at $\sim 5.8R_g$. Encouragingly, this is almost exactly where the neutron star surface is expected to be.

3 TESTING LENSE-THIRRING IN ATOLLS

Now we have both the inner and outer radius for the hot flow, we can directly test our model for the LF QPO. The inner radius in this model is set by the increase in stress from the torque produced by the misaligned flow leading to a drop in the surface density of the hot flow. This torque is communicated by bending waves, and gets larger for larger spins, so that the effective inner radius of the flow increases with a_* , unlike the last stable orbit. This cancels out a large part of the predicted spin dependence of Lense-Thirring precession, giving a much better match to the data (IDF09). The inner radius predicted from the bending waves is $\sim 3(h/r)^{-4/5} a_*^{2/5} \sim 5.7R_g$ for $a_* = 0.2$. This is also very close to the expected position of the last stable orbit and the expected size scale of the neutron star. While it is not clear quite which one of these three physical processes determines r_i , the fact that they are all so similar to each other and to the value derived above from the data is extremely encouraging.

The red line in Figure 4 shows LF QPO frequency predicted

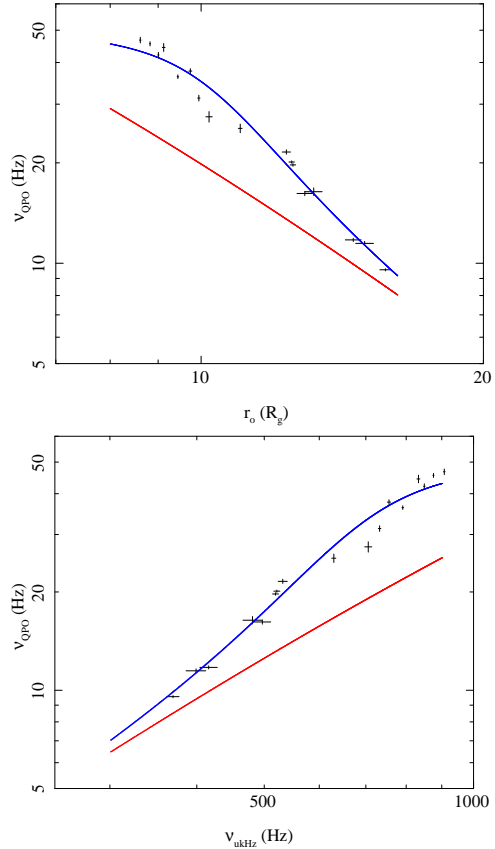


Figure 4. Theoretical and observed LF QPO frequency plotted against r_o (top) and ν_{ukHz} (bottom). The lines represent theoretical data where the LF QPO is assumed to be the result of Lense-Thirring precession of a flow with surface density $\Sigma = \Sigma_o(r/r_i)^{-\zeta}$. The red line is for $\zeta = 0$ as this is what is found in simulations for BHB. The blue line represents the case where the surface density profile changes according to the phenomenological model illustrated in Figure 5.

by the model of IDF09 using this inner radius and the inferred outer truncation radius from the ukHz QPO. These match the data rather well at the the largest truncation radii (lowest luminosity, lowest frequencies) but diverge increasingly at smaller radii. The lower panel shows this in a slightly different way by plotting the LF QPO against the ukHz QPO frequency.

This could simply mean that the LF QPO does not originate in Lense-Thirring precession. However, there is one more parameter in the model of IDF09 which determines the LF QPO frequency, and that is the surface density, Σ , of the flow. IDF09 assumed $\Sigma = \Sigma_o(r/r_i)^{-\zeta}$ with $\zeta = 0$ between r_o and r_i . This is a good representation of the simulation data for BHB (e.g. Fragile et al 2007). However, neutron stars have a solid surface so the flow in atolls may become increasingly dense and increasingly concentrated on the neutron star surface as the accretion rate increases. Certainly, the spectral evolution shows that the boundary layer emission changes from optically thin to optically thick across these data. This effectively means that ζ should be increasing as ν_{ukHz} increases. Figure 5 shows a phenomenological model for the changing surface density profile. The blue line in Figure 4 traces the precession frequency for a flow with the surface density profile shown in Figure 5 and we see excellent agreement with observations.

Thus the atoll systems are not such a clean test of the LF QPO model as was originally hoped. A simple application of the model

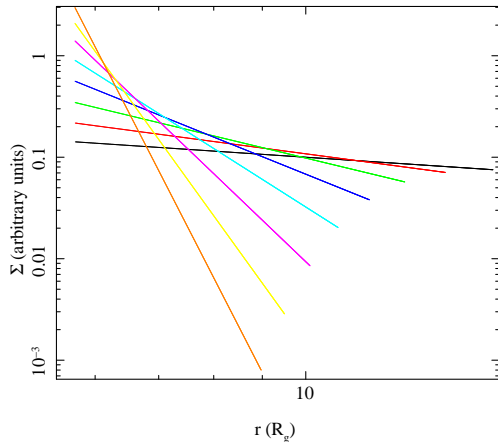


Figure 5. Plot showing the changing surface density profile required to give the precession frequency depicted by the blue line in Figure 4. The black line shows the surface density profile when $\nu_{ukHz} = 370$ Hz ($r_o \sim 16$) with the red, green, blue, cyan, magenta and yellow lines representing a ν_{ukHz} frequency 70Hz higher than the previous with the orange line representing the surface density when $\nu_{ukHz} = 860$ Hz ($r_o \sim 9$).

clearly fails, but it is entirely plausible that this is mainly due to the fundamental difference between atolls and BHB, namely the solid surface in the neutron stars causing a changing surface density profile in the hot flow.

4 CONCLUSIONS

We show that the broadband continuum noise power and LF QPO seen in atolls and BHB can be self-consistently explained in the *same* truncated disc/hot inner flow model which describes their spectral evolution. We test this on the atoll systems, as these have strong kHz QPOs which most probably pick out the truncation radius of the thin disc, r_o , so this key parameter is known independently. Using the standard assumption that the upper of the two kHz QPOs marks the Keplerian frequency gives that r_o decreases from $20 - 8 R_g$ during the marked spectral transition seen in atolls from the hard (island) state to soft (banana branch) spectra.

The low frequency break seen in the noise power is then consistent with being the viscous timescale of the hot flow at r_o . This requires that $\alpha(h/r)^2$ increases as r_o decreases, as seen in numerical simulations of the flow in BHB. All smaller radii in the hot flow contribute to the noise power, giving the broad band continuum power spectrum. The highest frequency noise component marks the viscous timescale at the inner edge of the hot flow, r_i . We use the values of $\alpha(h/r)^2$ determined from r_o to calculate r_i . This remains remarkably constant at $\sim 6 R_g$ (consistent with either the size scale of the neutron star, the last stable orbit, or the bending wave radius).

The truncated disc model also gives a physical interpretation for the observed ‘splitting’ of the lowest frequency noise component seen close to the spectral transition. At this point the spectral models predict that the disc overlaps the hot flow, so there is a component which tracks turbulence in the hot flow *within* the disc inner radius, and another component which tracks the true outer edge of the hot flow which extends over the disc.

With all of the parameters of the truncated disc geometry constrained, we are then able to test the Lense-Thirring precession model for the LF QPO presented in IDF09. However, there is still one additional free parameter which is the radial dependence of the surface density of the hot flow. Assuming that this has the

same form as in BHB gives a predicted LF QPO frequency which matches with the data at large radii, but increasingly diverges at smaller radii. However, it seems quite plausible that the solid surface of a neutron star makes a fundamental difference, with the flow increasingly piling up close to the neutron star. We show an example surface density based on this idea which can match the observed LF QPO frequency with Lense-Thirring precession of the hot flow. While we stress that simulations are required to independently test this phenomenological description, the fact that a solution can be found is very encouraging.

Overall, we present the first model of the power spectrum in which both broad band continuum and LF QPO components are interpreted physically. This forms a framework in which the characteristic frequencies in the power spectrum can be used as a diagnostic of the properties of the accretion flow in strong gravity.

5 ACKNOWLEDGEMENTS

AI acknowledges the support of an STFC studentship.

REFERENCES

- Altamirano D., van der Klis M., Méndez M., Jonker P. G., Klein-Wolt M., Lewin W. H. G., 2008a, *ApJ*, 685, 436
 Altamirano D., van der Klis M., Méndez M., Wijnands R., Markwardt C., Swank J., 2008b, *ApJ*, 687, 488
 Balbus S. A., Hawley J. F., 1998, *RvMP*, 70, 1
 Barret D., 2001, *AdSpR*, 28, 307
 Barret D., Olive J. F., Boirin L., Done C., Skinner G. K., Grindlay J. E., 2000, *ApJ*, 533, 329
 Barret D., Olive J.-F., Miller M. C., 2005, *AN*, 326, 808
 Belloni T., Psaltis D., van der Klis M., 2002, *ApJ*, 572, 392
 Cabanac R. A., Valls-Gabaud D., Lidman C., 2008, *MNRAS*, 386, 2065
 Chaty S., Haswell C. A., Malzac J., Hynes R. I., Shrader C. R., Cui W., 2003, *MNRAS*, 346, 689
 Churazov E., Gilfanov M., Revnivtsev M., 2001, *MNRAS*, 321, 759
 Done C., Gierliński M., Kubota A., 2007, *A&ARv*, 15, 1
 Fragile P. C., Mathews G. J., Wilson J. R., 2001, *ApJ*, 553, 955
 Fragile P. C., Blaes O. M., Anninos P., Salmonson J. D., 2007, *ApJ*, 668, 417
 Fragile P. C., Lindner C. C., Anninos P., Salmonson J. D., 2009, *ApJ*, 691, 482
 Gierliński M., Done C., Page K., 2008, *MNRAS*, 388, 753
 Gierliński M., Nikolajuk M., Czerny B., 2008, *MNRAS*, 383, 741
 Ingram A., Done C., Fragile P. C., 2009, *MNRAS*, 397, L101
 Klein-Wolt M., van der Klis M., 2008, *ApJ*, 675, 1407
 Krolik J. H., Hawley J. F., 2002, *ApJ*, 573, 754
 Lyubarskii Y. E., 1997, *MNRAS*, 292, 679
 Méndez M., 2006, *MNRAS*, 371, 1925
 Miller M. C., Lamb F. K., Cook G. B., 1998, *ApJ*, 509, 793
 Misra R., Zdziarski A. A., 2008, *MNRAS*, 387, 915
 Piro A. L., Bildsten L., 2005, *ApJ*, 629, 438
 Psaltis D., Belloni T., van der Klis M., 1999, *ApJ*, 520, 262
 Psaltis D., Norman C., 2000, *astro*, arXiv:astro-ph/0001391
 Remillard R. A., McClintock J. E., 2006, *AAS*, 38, 903
 Schnittman J. D., 2005, *ApJ*, 621, 940
 Stella L., Vietri M., 1998, *ApJ*, 492, L59
 Strohmayer T. E., Markwardt C. B., Kuulkers E., 2008, *ApJ*, 672, L37
 Sunyaev R., Revnivtsev M., 2000, *A&A*, 358, 617
 Titarchuk L., Shaposhnikov N., Arefiev V., 2007, *AIPC*, 910, 334
 van der Klis M., 2005, *Compact Stellar X-Ray Sources*, eds. W.H.G. Lewin and M. van der Klis, Cambridge University Press:astro-ph/0410551
 van der Klis M., Swank J. H., Zhang W., Jahoda K., Morgan E. H., Lewin W. H. G., Vaughan B., van Paradijs J., 1996, *ApJ*, 469, L1

6 *A. Ingram & Chris Done*

van Straaten S., van der Klis M., di Salvo T., Belloni T., 2002, *ApJ*, 568,
912

Wijnands R., van der Klis M., 1999, *ApJ*, 514, 939